I. Chan Chiang
Yu-Ting Kuo
Chia-Ying Lu
Kwok-Wan Yeung
Wei-Chen Lin
Feng-O. Sheu
Gin-Chung Liu

Distinction between high-grade gliomas and solitary metastases using peritumoral 3-T magnetic resonance spectroscopy, diffusion, and perfusion imagings

I. C. Chiang · Y.-T. Kuo · C.-Y. Lu
K.-W. Yeung · W.-C. Lin
F.-O. Sheu · G.-C. Liu (✉)
Department of Radiology,
Chung-Ho Memorial Hospital,
Kaohsiung Medical University,
No. 100 Shih-Chuan 1st Road,
Kaohsiung, Taiwan
E-mail: ugarte1735@yahoo.com.tw
Tel.: +886-7-3208235
Fax: +886-7-3154208

Abstract This study compared the effectiveness of relative cerebral blood volume, apparent diffusion coefficient, and spectroscopic imaging in differentiating between primary high-grade gliomas and solitary metastases. A 3.0-T MR unit was used to perform proton MR spectroscopy, diffusion imaging, and conventional MR imaging on 26 patients who had solitary brain tumors (14 high-grade gliomas and 12 metastases). All diagnoses were confirmed by biopsy. Twelve perfusion MR studies (8 high-grade gliomas and 4 metastases) were also performed. The results showed that the choline to creatine ratio and relative cerebral blood volume in the peritumoral regions of high-grade gliomas were significantly higher than they were in the metastases. The apparent diffusion coefficient values in tumoral and peritumoral regions of metastases were significantly higher than they were in the primary gliomas. Although conventional MR imaging characteristics of solitary metastases and primary high-grade gliomas may sometimes be similar, the peritumoral perfusion-weighted and spectroscopic MR imaging enable distinction between the two. Diffusion-weighted imaging techniques were complementary techniques to make a differential diagnosis between the two malignant tumors.

Keywords High-grade glioma · Solitary metastasis · Diffusion · Perfusion · Spectroscopy

Introduction

In vivo magnetic resonance (MR) spectroscopy techniques, including single-voxel MR spectroscopy [1, 2, 3] and the more advanced MR spectroscopic imaging [4, 5], are noninvasive techniques that provide information about the metabolic characteristics of tissue in the brain. These studies have shown that MR spectroscopy is valuable for distinguishing active tumor from normal tissue or edema. This suggests that MR spectroscopy may be important in defining the spatial extent and characteristics of tumors. Diffusion and perfusion MR imaging has also been used for evaluating intracranial tumors [6, 7].

Intracranial metastases and primary high-grade gliomas are two types of brain tumors commonly encountered in the adult population. The management of these two tumors is different and can potentially affect the clinical outcome. In many cases the two entities cannot be differentiated by using conventional MR imaging. In peritumoral edema of primary high-grade gliomas it has been reported to have peritumoral infiltrating neoplastic cells [8]. Therefore the tumor border is still inaccurately depicted even with conventional MR imaging. Because our initial observations of high-grade gliomas have revealed a good correlation between apparent diffusion coefficient (ADC) with tumor cellularity and vasogenic edema,

we expanded our study to include the metastatic tumors.

Advanced MR imaging techniques are used to obtain metabolic information that complements the anatomical images provided by conventional MR imaging. The perfusion-weighted MR imaging provides noninvasive measurements of tumor vascularity. Relative cerebral blood volume (rCBV) maps derived from perfusion-weighted MR can be used to quantify areas of neovascularization. Perfusion MR imaging has become an important means of characterizing intracranial neoplasms [9].

In vivo MR spectroscopy provides metabolic information about brain tumors [10]. The limited spatial and spectral resolution at the standard magnetic field of 1.5 T are overcome in a higher field strength 3 T scanner due to improved spectral resolution and increased signal to noise ratio (SNR). The improved spectral resolution provides separation of metabolite signals and thereby improves the ability to distinguish among tumor, normal brain tissue and nonviable tissues, including edema, gliosis, and necrosis [11, 12]. This distinction is provided by the relative levels of choline (Cho), creatine (Cr), and N-acetylaspartate (NAA). Decreased NAA and elevated Cho are associated with tumor tissue.

The purpose of this study was to investigate the potential roles of 3-T MR spectroscopy, rCBV, and ADC in distinguishing between primary high-grade gliomas and solitary metastases on the basis of differences in vascularity, water self-diffusion and metabolite levels in the tumor, and peritumoral regions.

Material and methods

Patients

In this prospective study carried out between March 2003 and November 2003 a 3.0-T MR unit was used to perform proton MR spectroscopy, diffusion imaging, and conventional MR imaging on 26 patients with solitary brain tumors (14 high-grade gliomas and 12 metastases). Twelve perfusion MR studies (8 high-grade gliomas and 4 metastases) were also performed. The 26 patients (12 men and 14 women; 25–76 years of age) with untreated solitary brain tumors underwent MR imaging. The presence of the high-grade glioma or metastases was histologically verified by means of either stereotactic biopsy or surgical resection. All of the 14 high-grade gliomas were glioblastoma multiforme. Of the 12 patients with biopsy-confirmed metastases all were carcinomas, 9 were from known primary (2 breast, 5 lung, 2 stomach) and 3 from an unknown primary site. Informed consent for MR examination was obtained from all patients.

▶

Fig. 1 Localizing image from axial T1-weighted images in a 46-year-old man with pathologically confirmed glioblastoma multiforme. **a** Localizing image from postcontrast axial T1-weighted MR demonstrates the voxel position at intratumoral region (*voxel 1*). There is elevation in Cho/Cr to 1.98. The voxel position at peritumoral region with corresponding spectrum (1000/144) demonstrates elevated Cho/Cr, 1.84, in keeping with tumoral infiltration in the peritumoral region (*voxel 2*). **b** There is elevation in peritumoral rCBV (*voxel 2*) to 122%, compared with intratumoral rCBV (*voxel 1*) and the contralateral normal white matter used as a control (*voxel 3*). The measured signal vs. time curves corresponding to the tumor and peritumoral voxel positions. The curves 1 and 2, corresponding to the voxels at the tumor and peritumoral regions, reveal increased enhancement of the signal after the bolus arrival

MR techniques

The MR imaging was performed with a 3-T Signa system (GE Medical Systems, Milwaukee, Wis., USA). A standard quadrature head coil (GE Medical Systems) was used for the all patients. Each MR examination included precontrast transverse T2- and T1-weighted spin-echo imaging followed by diffusion-weighted images. The perfusion-weighted imaging and MR spectroscopy were performed after contrast material administration. In each study T2-weighted images were acquired using a spin echo sequence with a TR/TE of 4000/100, a slice thickness of 3 mm and field of view of 240×180. Precontrast T1-weighted images were then acquired with a slice thickness of 3 mm and a TR/TE of 800/9 (Fig. 1). Postcontrast axial images were obtained after perfusion-weighted images. Subsequent diffusion-weighted and spectroscopic imaging were also performed.

For perfusion-weighted imaging a series of T2-weighted gradient-echo-planar images were obtained during the first pass of a bolus of contrast material, at a dose of 0.1 mmol/kg body weight. The section thickness and location of the perfusion-weighted MR data set were determined by using the axial T2-weighted images to locate the lesion and the peritumoral T2 signal abnormality. Region of interest (ROI) size was 2–5 mm in diameter (depending on the size of the lesion) and was placed based on the color overlap maps.

Spectroscopy

Spectroscopic data were obtained after gadopentetate dimeglumine administration. two-dimensional chemical shift imaging (2D-CSI) was performed in all patients. For the 2D-CSI technique a data set was obtained from a selected volume of 18–135 cm^3 (minimum 3×4×1.5 cm; maximum 10×9×1.5 cm) by using a spin-echo sequence with phase-encoding gradients in two directions, automatic shimming, and gaussian water suppression. Measurement parameters used in 2D-CSI
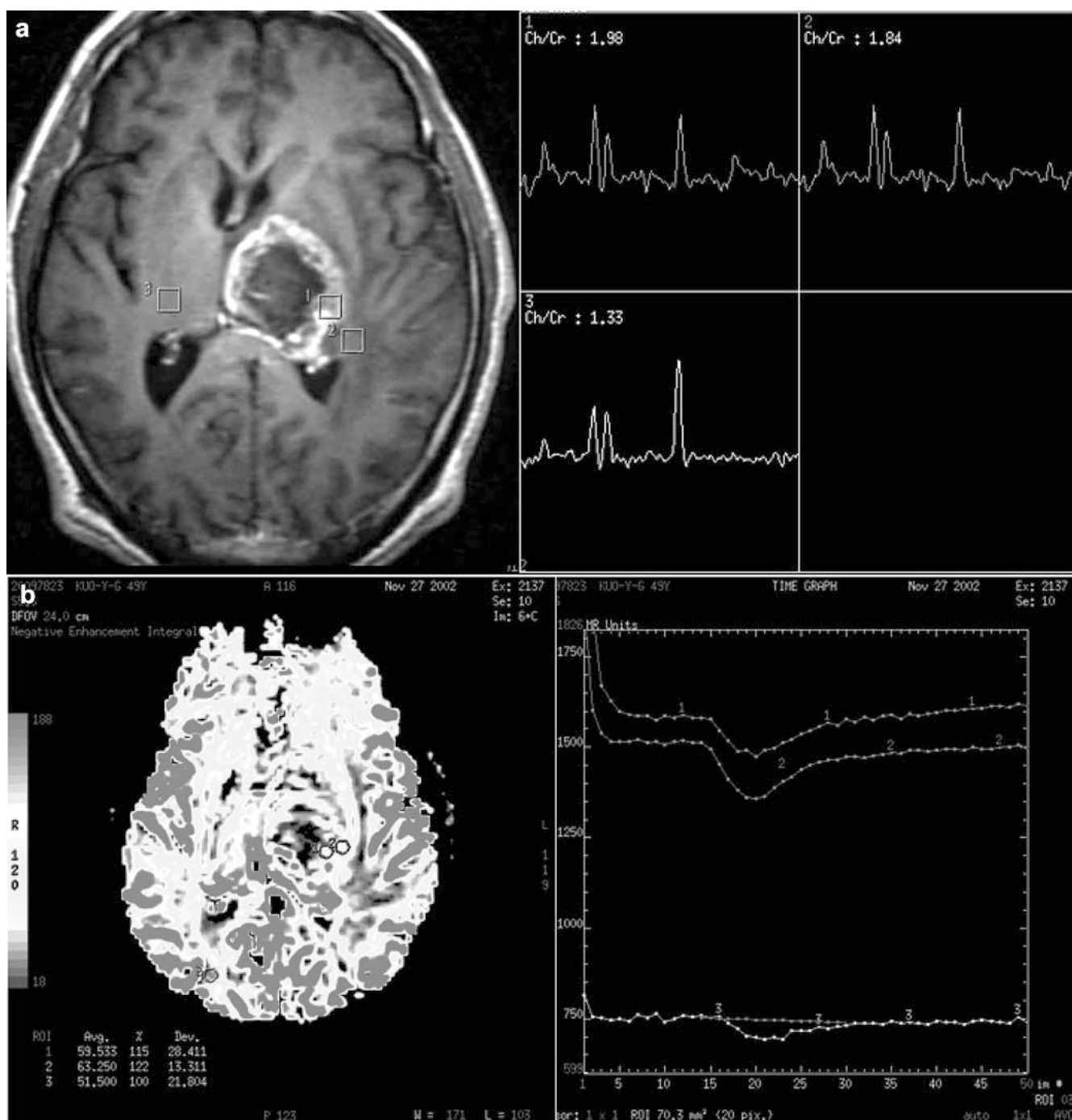
were 1500/270/2 (TR/TE/excitations), 16×16 phase-encoding steps, 160×160 mm field of view, 15 mm section thickness, and 1024 data points. Data sets of 1.5 cm³ resolution were acquired within 12 min (6 min in the six measurements with one excitation). The rectangular spectroscopic ROI was localized by using the transverse T1-weighted 3-T MR images, and the size ranged from 1×1×1 to 1×1×1.5 cm. Total

examination time, including setup, was approx. 1 h. The section was positioned to include the enhancing lesion, peritumoral region, and a normal contralateral brain parenchyma as a control.

Diffusion imaging was performed in the transverse plane by using a spin-echo echo-planar imaging sequence with the following parameters: repetition time (ms)/echo time (ms)/inversion time (ms), 12,000/100/

2,200; diffusion gradient encoding in three orthogonal directions; $b = 1,000$ s/mm^2, field of view 20×40 cm, matrix size 128×64 pixels, section thickness 5 mm, section gap 2.5 mm, and number of signals acquired, 1. After pixel-by-pixel calculation an ADC map was obtained. The ADC values were then calculated by manually placing circular ROIs in the enhancing lesion, peritumoral region, and a normal contralateral brain parenchyma as a control, guided by T2-weighted and contrast-enhanced images. Each measurement was performed by using ROI areas (average ROI 2 ± 5 mm).

Data processing

For perfusion-weighted imaging the MR data were processed as previously described by Knopp et al. [13]. The peritumoral region was defined to be within 1 cm outside the outer enhancing tumor margin. The rCBV values were then measured in three ROIs within each area of the peritumoral region and within the enhancing tumor. Maximal rCBV values were obtained by identifying regions of maximal perfusion from color maps. The full calculation of relative CBV outlined above was then applied to ROIs over these regions, expressed relative to values measured in contralateral white matter.

Spectroscopy

The in vivo MR spectroscopic data were analyzed on a Sun Ultra 1 workstation (Sun Microsystems, Mountain View, Calif., USA) by using Sage IDL processing software (GE Medical Systems). The spectral data were baseline corrected, apodized, filtered, and Fourier transformed. Since there were three-dimensional acquisitions, the spectra could be reconstructed to coincide with the ROI specified in three dimensions by using these programs. Gaussian curves were fitted to Cho, Cr, and NAA peaks and peak area ratios (Cho/Cr and NAA/Cr) were calculated. Spectra with no significant NAA, Cr, or Cho resonances (less than 3 SD of the noise values) were assumed to correspond to nonviable tissue. Metabolic ratios were calculated in the multiple voxels; however, only the maximal values in the three locations (within the enhancing tumor, the peritumoral region, and normal contralateral brain parenchyma) were included. Metabolite values were calculated automatically from the area under each metabolite peak by using the standard commercial software program provided by the manufacturer. Peak integral values were normalized to the internal Cr peak.

Diffusion-weighted imaging

Standard mean ADC values were calculated automatically and expressed as 10^{-3} mm^2/s.

Statistical analysis

rCBV (ml/100 g) from perfusion, ADC ($\times 10^{-9}$ m^2/s) from diffusion, and metabolites ratios on CSI MR imaging were measured in the contrast-enhancing tumor and peritumoral regions. The rCBV measurements were obtained from the perfusion-weighted MR data, and Student's t test was used to determine the statistical difference in rCBV between high-grade gliomas and metastases. Metabolic ratios obtained from spectroscopic MR imaging data between high-grade gliomas and metastases were compared by using Student's t test. This test was also used to determine whether there was a statistically significant difference in ADC values between the metastases and high-grade gliomas. A P value less than 0.05 was considered to be statistically significant different.

Results

The ADC values measured in the tumors and the surrounding edema are shown in Table 1. The ADC values in tumor regions (high-grade gliomas 1.04 ± 0.42, metastases 1.87 ± 0.73, $P < 0.005$) and ADC in peritumoral regions (high-grade gliomas 2.01 ± 0.37, metastases 2.41 ± 0.33, $P < 0.05$) were calculated. High ADC values were identified in cystic and necrotic areas. In the peritumoral edema of metastases and high-grade gliomas the ADC were higher than those in contrast enhancing tumor. We found the mean ADC values at contrast-enhancing areas and peritumoral edema of metastases to be significantly higher than those in high-grade gliomas. Table 1 also summarizes the results of the rCBV values. Our main findings reveal statistically significant differences in the rCBV in peritumoral region (high-grade gliomas 2.33 ± 1.61, metastases 0.84 ± 0.33, $P < 0.005$). The Cho/Cr ratio in peritumoral region in high-grade gliomas and metastases was 1.30 ± 0.45 and 0.29 ± 0.51 respectively ($P < 0.001$). The intratumoral rCBV, Cho/Cr, NAA/Cr, and peritumoral NAA/Cr

Table 1 Diffusion MR ADC values, perfusion MR rCBV values and Cho/Cr ratios

Location/technique	Glioma ($n = 14$)	Metastases ($n = 12$)	P [a]
Tumoral ADC	1.04 ± 0.42	1.87 ± 0.73	< 0.005
Peritumoral ADC	2.01 ± 0.37	2.41 ± 0.33	< 0.05
Tumoral rCBV	0.09 ± 0.05	0.22 ± 0.23	> 0.05
Peritumoral rCBV	2.33 ± 1.61	0.84 ± 0.33	< 0.005
Tumoral Cho/Cr	1.82 ± 0.66	1.55 ± 0.74	> 0.05
Peritumoral Cho/Cr	1.30 ± 0.45	0.29 ± 0.51	< 0.001
Tumoral NAA/Cr	0.45 ± 0.08	0.47 ± 0.02	> 0.05
Peritumoral NAA/Cr	0.69 ± 0.08	0.72 ± 0.16	> 0.05

[a] Student's t test

ratios in high-grade gliomas did not differ statistically from those seen with metastases (Table 1). Within the enhancing portion of the cerebral metastases lipids (at 0.9 ppm) and lactate (at 1.35 ppm) were detected (Fig. 2a; see also Fig. 3).

Discussion

Gliomas are the most common brain tumors. On imaging studies malignant gliomas are usually enhanced after intravenous contrast administration and show peritumoral edema, whereas, except for pilocytic astrocytoma, low-grade gliomas usually show little to no abnormal contrast enhancement and peritumoral edema [13]. The brain is a frequent site of hematogeneous metastases from malignant tumors in other organs. Along with primary glial tumors in the brain, metastases are associated with high morbidity and mortality. The approach to imaging diagnosis, treatment and follow-up is different between the two pathological conditions. Since conventional MR imaging is limited in its ability to distinguish high-grade gliomas from metastatic tumors, the urgency of new and more advanced techniques that can better detect neoplastic cell infiltration in the peritumoral regions is important.

Absolute ADC measured in intracranial tumors had been rarely reported until recently. Tien et al. [14] reported ADC in ten patients with high-grade gliomas using an echo-planar MR imaging method, measuring ADC along the cephalocaudal axis in a single coronal slice. Brunberg et al. [15] reported 40 patients with cerebral gliomas, using a motion insensitive line scanning spin-echo sequence measuring ADC along the three Cartesian axes. The study reported by Lu et al. [16] confirmed statistically significant changes between the mean diffusivity and fractional anisotropy values of normal-appearing white matter and those of the peritumoral T2 signal intensity abnormality. Surrounding both gliomas and metastatic lesions, there was an increase in mean diffusivity and a decrease in fractional anisotropy, which are best explained by increased extracellular bulk water.

We found the mean ADC values at contrast-enhancing areas and peritumoral edema of metastases to be significantly higher than those in high-grade gliomas. This finding may help to distinguish preoperatively between high-grade gliomas and metastases. The higher ADC in metastases suggests higher intracellular and extracellular water fractions than in high-grade gliomas. The significantly increased ADC in edema surrounding metastases suggests that they cause more fluid production than high-grade gliomas [17]. Malignant gliomas have neoplastic cells in the peritumoral edema. We hypothesized that ADC values could delineate areas of neoplastic cell infiltration. Indeed, Tien et al. [14] was able to distinguish areas of peritumoral neoplastic cell infiltration from predominantly peritumoral edema when abnormalities were located in the white matter aligned in the direction of the diffusion-weighted gradient. Our findings support the hypothesis that the peritumoral neoplastic cell infiltration can be depicted by ADC values. In our prospective study we found that rCBV and Cho/Cr ratios obtained from the peritumoral areas of solitary metastasis and primary gliomas differ significantly. These findings are consistent with known pathophysiological findings.

The T2-weighted areas of hyperintensity seen in peritumoral regions surrounding metastases is likely due to vasogenic edema associated with the abnormally leaking capillaries [18]. Furthermore, animal studies have shown that blood flow in edematous tissue is decreased due to local compression of the microcirculation by extravasated fluid [19]. These two factors may account for the decrease in rCBV in the peritumoral region of metastases. Within the peritumoral regions of high-grade gliomas the T2 hyperintensity is at least partially due to tumor infiltration [20]. This finding may explain the increase in rCBV. For rCBV values to be useful it must be shown that rCBV above that of normal white matter corresponds to tumor presence [21].

Cho is known to increase in the presence of increased membrane turnover and cellular proliferation and should be elevated in peritumoral areas of high-grade gliomas [22]. Our findings show that the measuring intratumoral Cho/Cr ratio is often not as useful as measuring the peritumoral Cho/Cr ratio to differentiate between high-grade gliomas and metastases. Most previous investigators have found no significant difference in the intratumoral spectra of metastases and high-grade gliomas, although a small number of early study findings suggest possible spectral differences between metastases and gliomas [11]. Bruhn et al. [23] reported a series of nine primary and metastatic tumors. It was shown that there was an increase in choline in both metastases and gliomas within the enhancing tumor, and the intratumoral spectra did not allow differentiation between the two tumor types. Our study differs in that we are investigating the peritumoral rather than intratumoral spectra and rCBV.

Additionally, spectral patterns with elevated Cho/Cr and decreased NAA/Cr ratios indicate tumor presence [24]. A combination of rCBV with proton spectra increases the effectiveness of these techniques in distinguishing tumor presence from vasogenic edema in the peritumoral regions. Of all the regions in which conventional MR imaging suggests possible tumor infiltration in the peritumoral region five cases had normal-appearing rCBV. Previous studies have indicated that normal-apperearing rCBV in high-grade gliomas corresponds to tumor infiltration with micronecrosis [25]. As a result of the heterogeneous rCBV values found in our
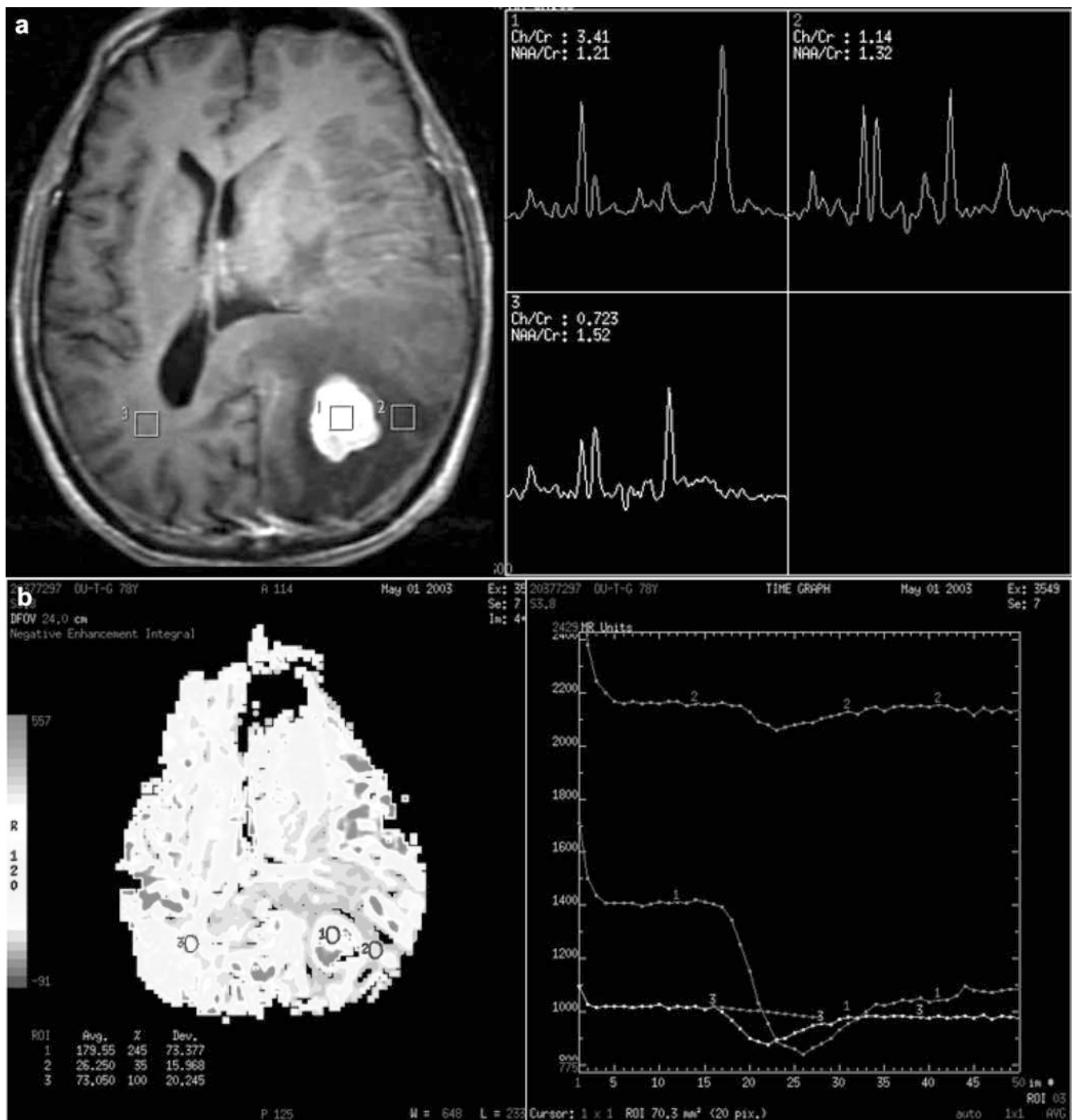
study for high-grade gliomas the average rCBV values in high-grade gliomas were not significantly higher than white matter values. Also, since the rCBV values of high-grade gliomas are typically between white and gray matter values, the sensitivity of rCBV in identifying tumor infiltration in the peritumoral regions is limited near the cerebral cortex and other regions that have rCBV values above normal white matter. The MR spectroscopy did not suffer from this limitation because the difference in metabolite levels between normal and tumor voxels is much greater than the difference between the metabolite levels in normal gray and white matter. On the other hand, the interpretation of spectra from regions with heterogeneous morphology and enhancement was difficult. In such cases it was not possible to determine wheter voxels with normal to minimally

◄

Fig. 2 Localizing image from postcontrast axial T1-weighted MR in a 74-year-old woman with a metastatic tumor from brochogenic carcinoma. **a** The voxels of interest on the three positions: *1* Intratumoral spectrum (1000/144), with the voxel in the tumor, demonstrates Cho/Cr elevation to 3.41 and NAA/Cr reduction. The spectrum of this metastatic tumor could not be differentiated from that of the high-grade glioma. *2* Peritumoral spectrum (1000/144) demonstrates no evidence of tumoral infiltration in peritumoral region. There is a diminution of Cho/Cr ratio to 1.14. *3* Spectrum (1000/144) in the contralateral normal white matter is included to ensure that the abnormal spectra are of diagnostic quality. **b** A left occipital lesion at color map (*left*). Peritumoral rCBV (*voxel 2*) is reduced to 35%, compared with voxel 3, in the contralateral normal white matter used as a control. The measured signal vs. time curves correspond to the three voxel positions (*right*). *Curve 2* at the peritumoral region reveals nonsignificant enhancement of the signal after the bolus arrival

increased Cho/Cr ratio correspond to peritumoral neoplastic cell infiltration or partial voluming of tumor and necrosis. In these circumstances the higher resolution of the rCBV color maps allowed the identification of peritumoral infiltration due to hypervascularity.

In our study the mean rCBV value in the peritumoral region of high-grade gliomas was statistically significantly higher than that of metastases, which suggests increased peritumoral perfusion due to tumor infiltration in the high-grade gliomas and compression of capillaries by vasogenic edema in the cases of metastatic tumors. The Cho/Cr ratio in peritumoral region of

Fig. 3 Regions of interest in the same cases of glioblastoma multiforme and metastases are shown. In the peritumoral edema of metastases and high-grade gliomas the ADC were higher than those in contrast enhancing tumor

high-grade gliomas was statistically significantly higher than that of metastases. Once again, this is consistent with peritumoral neoplastic cell infiltration in the high-grade gliomas. However, there was no significant difference in peritumoral NAA/Cr between the two groups because there is no neuronal replacement or destruction in the peritumoral regions of either pathological condition. In high-grade gliomas tumor cells infiltrate along vascular channels but do not destroy the preexisting cytoarchitecture [8]. There was also no appreciable difference in the tumoral NAA/Cr between the two tumor types. Within the enhancing portion of a cerebral metastases from bronchogenic carcinoma lipids (at 0.9 ppm) and lactate (at 1.35 ppm) were detected. The lipids have been shown to be related to necrosis and cell breakdown, and are typically associated with malignant tumors [26]. These metabolites did not serve to differentiate between high-grade gliomas and metastases.

Many studies on in vivo MR spectroscopy use a the voxel size of 8 cm^3 or larger [27, 28, 29, 30]. The 3-T data obtained in the present study suggest that this degree of spatial resolution is not adequate for characterizing heterogeneous tumor beds. Because of the improved spectral resolution and gain in SNR we used a higher than standard magnetic field of 1.5 T imager to determine the cell type of brain tumor. The twofold improvement in SNR at 3 T compared with that at 1.5 T allowed the use of a 10-mm section thickness (rather than the usual 15–20 mm) and an in-plane resolution as small as 0.75 (32×32 phase-encoding matrix) while maintaining an SNR of 5–6 for Cr_n. The voxel position is crucial in all cases of solitary brain tumors when
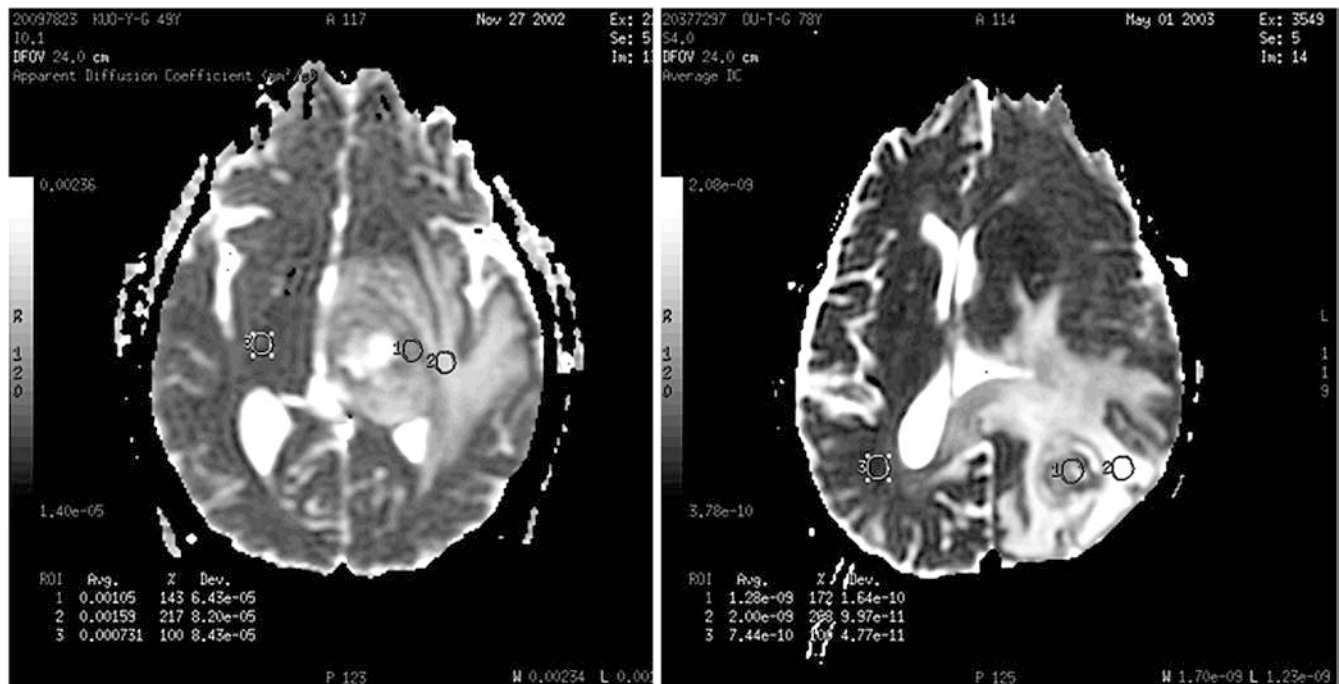
single-voxel spectroscopy is used [31]. The voxels on the normal-appearing brain parenchyma are used as control and increases the likelihood of demonstrating the most metabolically active portion of the tumor [32].

In conclusion, spectroscopic and perfusion-weighted MR imaging are advanced MR techniques that are used add important physiological and metabolic information to that obtained with conventional MR imaging. This study demonstrates that perfusion-weighted and spectroscopic MR measurements in the peritumoral region can be used to demonstrate differences in solitary metastases and high-grade gliomas. We strongly suggest the use of a combination of the two diagnostic procedures. The ADC values can be used to determine tumor type reliably and our results support the hypothesis that ADC values can detect neoplastic cell infiltration in peritumoral edema in patients with high-grade gliomas. The ADC values are complementary techniques to differentiate between the two pathological conditions. The intratumoral rCBV, Cho/Cr, NAA/Cr, and peritumoral NAA/Cr ratios in high-grade gliomas do not differ statistically from those seen with metastases.

References

1. Kaminogo M, Ishimaru H, Morikawa M et al. (2001) Diagostic potential of short echo time MR spectroscopy of gliomas with single-voxel and point-resolved spatially localized proton spectroscopy of brain. Neuroradiology 43:353–363
2. Luyten PR, Marien AJ, Heindel W et al. (1990) Metabolic imaging of patients with intracranial tumors: H-1 MR spectroscopic imaging and PET. Radiology 176:791–799
3. Alger JR, Frank JA, Bizzi A et al. (1990) Metabolism of human gliomas: assessment with H-1 MR spectroscopy and F-18 fluorodeoxyglucose PET. Radiology 177:633–641
4. Nelson SJ, Huhn S, Vigneron DB et al. (1997) Volume MRI and MRSI techniques for the quantitation of treatment response in brain tumors. Magn Reson Imaging 7:1146–1152
5. Vigneron DB, Bollen A, McDermott M et al. (2001) Three-dimensional magnetic resonance spectroscopic imaging of histologically confirmed brain tumors. Magn Reson Imaging 19:89–101
6. Krabbe K, Gideon P, Wagn P, Hansen U, Thosem C, Madsen F (1997) MR diffusion imagng of human intracranial tumors. Diagn Neuroradiol 39:483–489
7. Roland G, Daniel B, Vigneron N et al. (2001) Comparison of relative cerebral blood volume and proton spectroscopy in patients with treated gliomas. AJNR Am J Neuroradiol 21:357–366
8. Kelly PJ, Daumas-Duport C, Kispert DB, Kall BA, Scheithauer BW, Illig JJ (1987) Imaging-based stereotaxic serial biopsies in untreated intracranial neoplasms. J Neurosurg 66:865–874
9. Henry RG, Vigneron DB, Fischbein NJ et al. (2000) Comparison of relative cerebral blood volume and proton spectroscopy in patients with treated gliomas. AJNR Am J Neuroradiol 21:357–366
10. Castillo M, Kwock L (1998) Proton MR spectroscopy of common brain tumors. Neuroimaging Clin N Am8:733–752
11. McBride DQ, Miller BL, Nikas DL et al. (1995) Analysis of brain tumors using 1H magnetic resonance spectroscopy. Surg Neurol 44:137–144
12. Shimuzu H, Kumabe T, Tominaga T et al. (1996) Non-invasive evaluation of malignat brain tumors wityh proton MR spectroscopy. AJNR Am J Neuroradiol 17:737–747
13. Knopp EA, Cha S, Johnson G et al. (1999) Glial neoplasms: dynamic contrast enhanced T2-weighted MR imaging. Radiology 211:791–798
14. Tien RD, Felsberg GJ, Friedman H, Brown M, McFall J (1994) MR imaging of high-grade cerebral gliomas: value of diffusion-weighted echoplanar pulse sequences. AJR Am J Roentgenol 162:671–677
15. Brunberg JA, Chenevert TL, MckeeverPE et al. (1995) In vivo MR determination of water diffusion coefficients and diffusion anisotropy: correlation with structural alteration in gliomas of cerebral hemispheres. AJNR Am J Neuroradiol 16:361–371
16. Lu S, Ahn D, Johnson G, Cha S (2003) Peritumoral diffusion tensor imaging of high- grade gliomas and metastatic brain tumos. AJNR Am J Neuroradiol 24:937–941
17. Steen RG (1992) Edema and tumor perfusion: characterization by quantitative proton MR imaging. AJR Am J Roentgenol 158:259–264
18. Zhang M, Olsson Y (1997) Hematogenous metastases of the human brain: characteristics of peritumoral brain changes—a review. J Neurooncol 35:81–89
19. Hossman KA, Bloink M (1981) Blood flow and regulation of blood flow in experimental peritumoral edema. Stroke 12:211–217
20. Burger P (1990) Classification, grading, and patterns of spread of malignant gliomas. In: Apuzzo ML (eds) Neurosurgical topics: malignant cerebral glioma. American Association of Neurological Surgeons, Park Ridge, 3–17
21. Aronen HJ, Gazit IE, Louis DN et al. (1994) Cerebral blood volume maps of gliomas: comparison with tumor grade and histologic findings. Radiology 191:41–51
22. Poptani H, Gupta RK, Roy R, Pandey R, Jain VK, Chhabra DK (1995) Characterization of intracranial mass lesions with in vivo proton MR spectroscopy. Am J Neuroradiol 16:1593–1603
23. Bruhn H, Frahm J, Gyngell ML et al. (1989) Noninvasive differentiation of tumors with use of localized H-1 MR spectroscopy in vivo: initial experience in patients with cerebral tumors. Radiology 172:541–548
24. Preul MC, Caramanos Z, Collins DL et al. (1996) Accurate, noninvasive diagnosis of human brain tumors by using proton magnetic resonance spectroscopy. Nat Med 2:323–325
25. Sugahara T, Korogi Y, Kochi M et al. (1998) Correlation of MR imaging-determined cerebral blood volume maps with histologic and angiographic determination of vascularity of gliomas. AJR Am J Roentgenol 171:1479–1486

26. Li X, Lu y, Pirzkall A, McKnight T, Nelson S (2002) Analysis of the spatial characteristics of metabolic abnormalities in newly diagnosed glioma patients. J Magn Reson Imaging 16:229–237

27. Ikehira H, Miyamoto T, Yasukawa T et al. (1995) Differences in metabolic and morphological reactions after radiation therapy: proton NMR spectroscopy and imaging of patients with intracranial tumors. Radiat Med 13:199–204

28. Usenius T, Usenius J, Tenhunen M et al. (1995) Radiation-induced changes in human brain metabolites as studied by 1H nuclear magnetic resonance spectroscopy in vivo. Int J Radiat Oncol Biol Phys 33:719–724

29. Walecki J, Sokol M, Pieniazek P et al. (1999) Role of short TE 1H-MR spectroscopy in monitoring of postoperation irradiated patients. Eur J Radiol 30:154–161

30. Taylor JS, Langston JW, Reddick WE et al. (1996) Clinical value of proton magnetic resonance spectroscopy for differentiating recurrent or residual brain tumor from delayed cerebral necrosis. Int J Radiat Oncol Biol Phys 36:1251–1261

31. Ricci PE, Pitt A, Keller PJ, Coons SW, Heiserman JE (2000) Effect of voxel position on single-voxel MR spectroscopy findings. AJR Am J Neuroradiol 21:367–337

32. Meng L, Soonmee C, Knopp EA, Johnson G, Arnett BS, Litt AW (2002) High grade-gliomas and solitary metasases: differentiaition by using perfusion and proton spectroscopic MR imaging. Radiology 222:715–721